

Phosphine–Imidazolyl Ligands for the Efficient Ruthenium-Catalyzed Hydrogenation of Carboxylic Esters

Kathrin Junge, Bianca Wendt, Felix Alexander Westerhaus, Anke Spannenberg, Haijun Jiao, and Matthias Beller*^[a]

Abstract: The synthesis of phosphine–imidazolyl ligands **1** and **2** in good yields is presented. In combination with $[\{\text{Ru}(\text{benzene})\text{Cl}_2\}_2]$, ligands **1c** and **1e** formed efficient catalyst systems for the selective hydrogenation of various carboxylic esters into their corresponding primary alcohols. Further-

more, the structures of four ruthenium complexes with ligands **1b**, **1c**, **1d**, and **1e** were determined by X-ray crystallography, which showed the formation

of different coordination modes depending on the ligand structure.

Keywords: alcohols • esters • hydrogenation • ligand design • ruthenium

Introduction

The reduction of esters into alcohols is one of the most-fundamental reactions in organic chemistry.^[1] Typically, this transformation is realized by using stoichiometric amounts of metal hydrides (LiAlH_4 , NaBH_4), thereby producing large quantities of waste. Obviously, from economic and ecological viewpoints, catalytic hydrogenation reactions offer an attractive alternative. However, until recently, the catalytic hydrogenation of esters,^[2] acids,^[3] and amides^[4] have only been scarcely explored and the full scope of these methods still need to be evaluated. In industry, heterogeneous catalysts (e.g., copper chromite) are typically used for this process under rather harsh conditions ($>200^\circ\text{C}$, 200 bar), which unfortunately limits their applications. Hence, the development of milder and more-selective methods by using molecular-defined catalysts is of significant interest for the fine chemicals and pharmaceutical industries. In pioneering work on the homogenous hydrogenation of esters, hydrido–ruthenate^[5a,b] salts or ruthenium–carbonyl clusters^[5c–f] were used as catalysts. Improved activity was reported with ruthenium–phosphine catalysts that were generated in situ from $[\text{Ru}(\text{acac})_3]$ (acac = acetylacetonate) and PR_3 .^[6] Since 2006, important advancements in the hydrogenation of carboxylic acid esters were achieved by Milstein

and co-workers,^[5g,k,l] Saudan et al.,^[5h] and others.^[5i,j] Encouraged by their elegant work, and owing to our own experiences in the hydrosilylation of various carboxylic acid derivatives,^[7] we became interested in investigating this type of reaction in more detail. Although the existing catalysts for ester reduction possess high efficiency and wide substrate scope, their functional-group tolerance is still limited. To tackle this problem, herein, we report the development of a modular built-up catalyst system that was based on ruthenium and phosphine–imidazolyl ligands (Figure 1); this system could be tailor-made for the hydrogenation of different types of carboxylic acid esters.

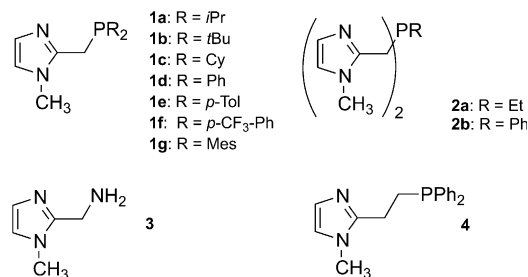


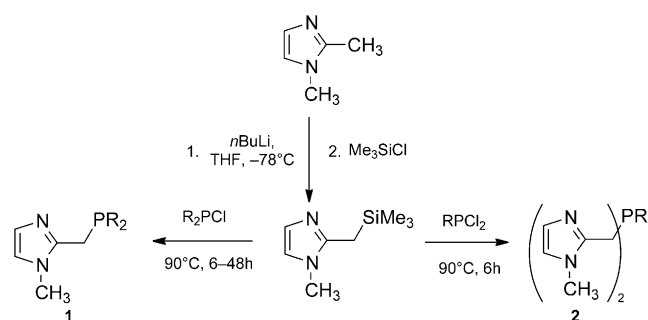
Figure 1. Structures of various phosphine/amine–imidazolyl ligands.

Results and Discussion

We began by preparing several new P–N ligands that contained phosphorous and imidazolyl nitrogen donor atoms in a straightforward two-step synthesis (Scheme 1). First, the lithiated 1,2-dimethylimidazole was selectively monosilylated at the 2-methyl position at -78°C to provide 1-methyl-[2-(trimethylsilyl)methyl]-1*H*-imidazole. Subsequent quenching with R_2PCl and RPCl_2 gave phosphine–imidazolyl ligands **1** and **2**, respectively, in good to excellent yields.^[8,9]

[a] Dr. K. Junge, B. Wendt, F. A. Westerhaus, Dr. A. Spannenberg, Dr. H. Jiao, Prof. Dr. M. Beller
Leibniz-Institut für Katalyse e.V. an der Universität Rostock
Albert-Einstein-Straße 29a, 18059 Rostock (Germany)
Fax: (+49) 381-1281-5000
Tel.: (+49) 381-1281-113
E-mail: Matthias.Beller@catalysis.de

Supporting information for this article is available on the WWW under <http://dx.doi.org/10.1002/chem.201200408>.



Scheme 1. Synthesis of phosphine-imidazolyl ligands **1** and **2**.

Owing to the large number of commercially available chlorophosphines, their aryl- and alkyl groups on the P-N ligands were modified to vary their steric and electronic properties. Apart from ligands **1a** and **1d**, which have already been reported in the literature, a range of new hemilabile P-N ligands were obtained in good to excellent yields.^[8a,b] To facilitate the purification process and for ease of handling, the hydrobromide salt was formed after distillation. Thus, the ligand salts were air- and moisture stable solids and could be stored for several months without any decomposition.

The molecular structures of ligands **1a**·2HBr and **1c**·HBr were confirmed by single-crystal X-ray diffraction analysis (Figure 2). In both structures, the hydrogen atom of HBr was coordinated to the unsubstituted nitrogen atom of the imidazole ring. In addition, the hydrogen atom of a second HBr molecule was associated with the phosphorous atom in structure **1a**.

Analogous phosphine-imidazolyl ligand **4**, which contained a two-carbon linker, was prepared according to a literature procedure (Scheme 2).^[8c,d] In this synthesis, 1-methylimidazol-2-yllithium was generated from the reaction of 1-methylimidazole and *n*-butyl lithium at -78°C followed by treatment with cyclic sulfate to form a lithium sulfate intermediate. The addition of LiPPh_2 led to displacement of the sulfate group by the PPh_2 moiety. Thus, compound **4** was prepared in high yield (85%) as a stable and easy to handle powder, whilst compound **3** was commercially available.^[10]

With a library of different P-N ligands in hand, we tested them in the ruthenium-catalyzed reduction of methyl benzoate (**5a**). For convenience, the $[\text{RuL}_2\text{Br}_2]$ catalyst was generated in situ from $[\text{Ru}(\text{cod})(\text{methylallyl})_2]$ (0.5 mmol) and ligands **1-4** (1 mmol).^[11] Initial studies on the influence of the experimental conditions on the reaction were carried out with ligand **1d** in the presence of base (10 mol%) in THF. To afford complete conversion within a reasonable length of time, the reaction was performed under 50 bar H_2 at 100°C (Table 1, entry 3). Benzyl alcohol (**6a**) was obtained in 88% yield after around 4 h. At 80°C , the conversion and yield of compound **6a** decreased dramatically and the formation of a significant amount of benzyl benzoate **7a** as a side-product, which was formed by the transesterification of methyl benzoate with benzyl alcohol, was observed (Table 1, entry 4).

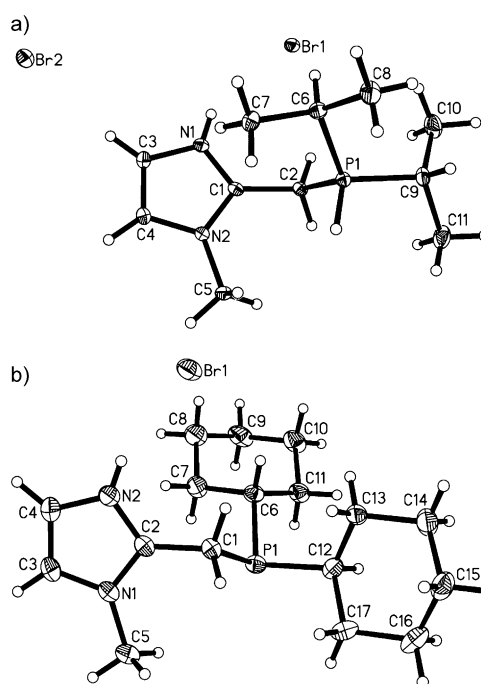
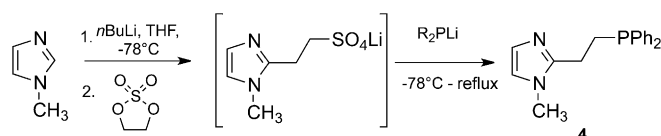


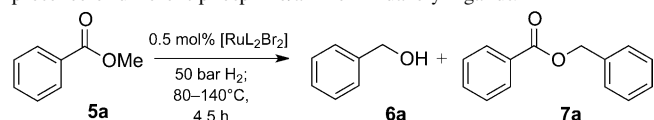
Figure 2. a) ORTEP of compound **1a**·2HBr; thermal ellipsoids set at 30% probability. Selected bond lengths [Å] and angles [°]: C2–P1 1.822(2), C6–P1 1.813(2), C9–P1 1.807(2); C2–P1–C6 112.09(11), C2–P1–C9 108.32(11), C6–P1–C9 113.11(10). b) ORTEP of compound **1c**·HBr; thermal ellipsoids set at 30% probability. Selected bond lengths [Å] and angles [°]: C1–P1 1.869(2), C6–P1 1.853(2), C12–P1 1.852(2); C1–P1–C6 102.26(10), C1–P1–C12 98.89(10), C6–P1–C12 103.87(10).



Scheme 2. Synthesis of 2-(2-(diphenylphosphino)ethyl)-1-methyl-1H-imidazole (**4**).

Next, we investigated the influence of the structure of the ligand on the catalytic activity for the reduction of methyl benzoate at 80°C by stepwise variation of the ligand pattern. As well as investigating different aryl and alkyl substituents on the phosphorous atom in ligands **1** and **2**, NH_2 -substituted derivative **3** and ligand **4**, which had an extended carbon chain, were also tested (Table 1). In the presence of imidazolyl ligands **2-4**, only low yields of benzyl alcohol (up to 30%) were obtained (Table 1, entries 11–14). Of the different ligands **1** examined, the highest product yield (92%) was achieved for ligand **1e** (Table 1, entry 8). In that case, a simple exchange of the phenyl ring with the electron-donating *p*-tolyl group at the phosphorous atom led to an increase in reactivity. Surprisingly, more-sterically demanding mesityl-substituted ligand **1g** showed a dramatic decrease in catalytic activity (Table 1, entry 10).

Furthermore, cyclohexyl-substituted ligand **1c** showed high efficiency for the reaction of methyl benzoate (Table 1,

Table 1. Ruthenium-catalyzed hydrogenation of methyl benzoate in the presence of different phosphine/amine–imidazolyl ligands.^[a]


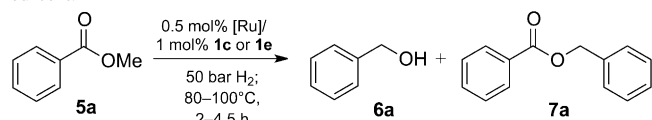
Ligand	<i>T</i> [°C]	Conversion [%]	Yield 7a [%]	Yield 6a [%]	
1	–	13	6	2	
2	1d	140	97	1	88
3	1d	100	>99	–	88
4	1d	80	37	10	13
5	1a	80	82	–	70
6	1b	80	30	10	9
7	1c	80	92	4	80
8	1e	80	99	<1	92
9	1f	80	56	15	37
10	1g	80	18	11	1
11	2a	80	37	14	8
12	2b	80	55	23	16
13	3	80	36	14	4
14	4	100	55	6	30

[a] Conditions: methyl benzoate (10 mmol), [RuL₂Br₂] (0.5 mol %), KO^tBu (10 mol %), THF (10 mL), 80–140 °C, H₂ (50 bar), 4.5 h. Catalyst preparation: [Ru(cod)(methylallyl)₂] (0.5 mmol), ligand **1–4** (1 mmol), and 3 equivalents HBr (0.29 M in MeOH) in acetone (1 mL) were stirred for 30 min, evaporated, and suspended in THF. cod = 1,5-cyclooctadiene.

entry 7). A number of different ruthenium precursors were also investigated with the two best ligands, **1c** and **1e** (Table 2), which led to the discovery of two efficient in situ catalyst systems. Whilst the combination [[Ru(benzene)Cl₂]₂]/**1e** was highly active in the reduction of substituted aromatic esters and lactones (Table 3), [[Ru(benzene)Cl₂]₂]/**1c** afforded especially good results with more-challenging substrates, such as aliphatic lactones or aliphatic carboxylic esters (Table 4).

The influence of various alkyl benzoates on the scope of the catalytic hydrogenation reaction was examined with the catalyst system [[Ru(benzene)Cl₂]₂]/**1e** (0.5 mol %; Table 3, entries 1–4). Whilst most of the substrates were smoothly reduced into their corresponding benzyl alcohols in high yields, the reduction of isopropyl benzoate only proceeded in a low yield. This result was in contrast to the findings of Saudan et al. who observed higher reactivity of isopropyl benzoate than other alkyl benzoates.^[5b] Furthermore, the tolerance of the reaction towards different functional groups was investigated. Good yields were achieved for aromatic esters that contained halide, ether, hydroxy, alkyl, and aryl substituents (Table 3, entries 5–11). However, cyano and ketone groups were preferentially reduced over the ester group.^[12] Notably, dicarboxylic esters and lactones were also reduced into their corresponding diols (Table 3, entries 12–14).

Finally, a series of aliphatic carboxylic esters and lactones was tested in the catalytic system [[Ru(benzene)Cl₂]₂]/**1c**. Their corresponding alcohols were formed in generally good yields (Table 4). α,β -Unsaturated esters gave their completely reduced products in up to 83% yield (Table 4, entries 4

Table 2. Hydrogenation of methyl benzoate with various ruthenium precursors.^[a]


[Ru]	Ligand	Conversion [%]	Yield 7a [%]	Yield 6a [%]	
1	[Ru(cod)(methylallyl) ₂]	1c	92	4	80
2	[Ru(cod)Cl ₂]	1c	68	11	48
3	[Ru(cod) ₂ BF ₄]	1c	53	8	32
4	[RuCl ₃ ·xH ₂ O]	1c	67	9	47
5	[[Ru(CO) ₃ Cl ₂]	1c	62	18	38
6	[Ru ₂ (CO) ₁₂]	1c	–	–	–
7	[[Ru(C ₃ H ₅)(CO) ₂]	1c	22	7	5
8	[Ru(C ₃ H ₅)(C ₁₀ H ₁₅)]PF ₆	1c	7	–	–
9	[Ru(acac) ₂ (cod)]	1c	6	4	–
10	[Ru(acac) ₃]	1c	58	13	38
11	[Ru(acac) ₂]	1c	–	–	–
12	[Ru(DMSO) ₄ Cl ₂]	1c	83	4	69
13	[Ru ₂ Cl ₂ (C ₁₀ H ₁₆) ₂]	1c	88	4	76
14	[[Ru(<i>p</i> -cymene)Cl ₂] ₂]	1c	97	2	88
15	[[Ru(benzene)Cl ₂] ₂]	1c	96	4	90
16 ^[b]	[[Ru(benzene)Cl ₂] ₂]	1c	97	1	92
17	[Ru(methylallyl) ₂ (cod)]	1e	99	<1	92
18	[[Ru(<i>p</i> -cymene)Cl ₂]	1e	49	23	17
19	[[Ru(benzene)Cl ₂]	1e	95	3	87
20 ^[c]	[[Ru(benzene)Cl ₂]	1e	77	7	74
21 ^[d]	[[Ru(benzene)Cl ₂]	1e	99	<1	94
22 ^[e]	[[Ru(benzene)Cl ₂]	1e	13	8	4
23 ^[b]	[Ru(C ₆ H ₆)Cl ₂ (1e)]	–	49	14	26
24 ^[f]	[Ru(C ₆ H ₆)Cl ₂ (1e)]	1e	98	1	83
25 ^[b]	[Ru(C ₆ H ₆)Cl(1c)]Cl	–	48	13	23
26 ^[f]	[Ru(C ₆ H ₆)Cl(1c)]Cl	1c	99	2	83

[a] Conditions: methyl benzoate (10 mmol), [Ru] (0.5 mol %), ligand **1c** or **1e** (1 mol %), KO^tBu (10 mol %), THF (10 mL), 80 °C, H₂ (50 bar), 4.5 h; [b] 100 °C, H₂ (50 bar), 2 h; [c] Ru/L = 1:1, 100 °C, H₂ (50 bar), 2 h; [d] Ru/L = 1:2, 100 °C, H₂ (50 bar), 2 h; [e] Ru/L = 1:4, 100 °C, H₂ (50 bar), 2 h; [f] [Ru(C₆H₆)Cl₂(**1**)] (0.5 mol %), **1** (0.5 mol %), KO^tBu (10 mol %), 100 °C, H₂ (50 bar), 2 h.

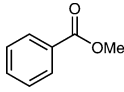
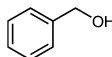
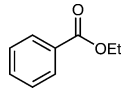
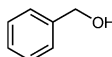
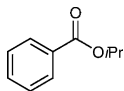
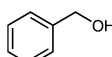
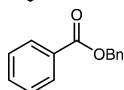
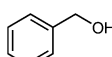
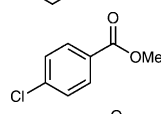
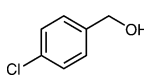
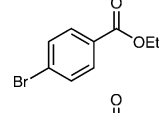
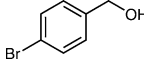
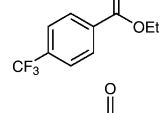
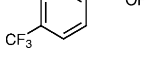
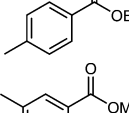
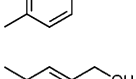
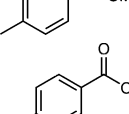
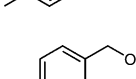
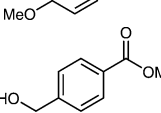
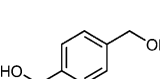
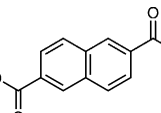
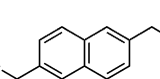
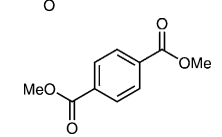
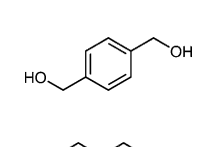
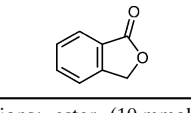
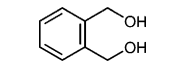
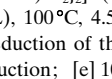
and 6), whilst cyclic lactones reacted to afford their corresponding diols in excellent yield (Table 4, entries 8 and 9).

As demonstrated in the initial experiments (Table 1) both in-situ-generated catalysts [[Ru(benzene)Cl₂]₂]/**1c** and [[Ru(benzene)Cl₂]₂]/**1e** were active for the reduction of methyl benzoate but the latter one showed higher efficiency for the reduction of aromatic esters. For comparison, the reduction of two aliphatic carboxylic esters were performed with [[Ru(benzene)Cl₂]₂]/**1e** (Table 4, entries 6 and 9) and moderate yields of the corresponding alcohols were obtained.

To get more information on the catalytic active species, crystals were grown from the catalyst solutions. To our delight, single crystals of [Ru(C₆H₆)Cl(**1b**)]Cl, [Ru(C₆H₆)Cl(**1c**)]Cl, [Ru(C₆H₆)Cl(**1d**)]Cl, and [Ru(C₆H₆)Cl₂(**1e**)] that were suitable for X-ray analysis were obtained by layering solutions of the complexes in CHCl₃ with *n*-pentane.

The ORTEPs of three cationic complexes, [Ru(C₆H₆)Cl(**1b**)]Cl, [Ru(C₆H₆)Cl(**1c**)]Cl, and [Ru(C₆H₆)Cl(**1d**)]Cl are shown in Figure 3 a–c. In all three of these structures, the nitrogen and phosphorus atoms of the P–N ligands were coordinated onto the metals, thus forming a five-membered

Table 3. Catalytic hydrogenation of aromatic carboxylic esters and lactones with $[\text{Ru}(\text{benzene})\text{Cl}_2]_2/\mathbf{1e}$.^[a]

	Ester	Alcohol	Yield [%]
1 ^[b]			94
2			99
3			44
4 ^[b]			99
5			92
6			24
7			17 84 ^[e]
8			66 ^[e]
9			49 58 ^[e]
10 ^[b]			66
11			80
12 ^[c]			31
13 ^[d]			67
14			64 83 ^[e]

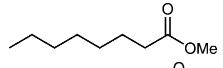
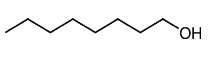
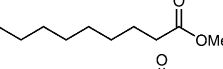
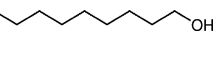
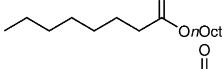
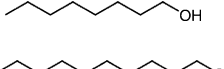
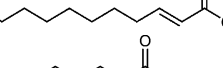
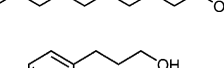
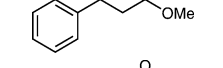
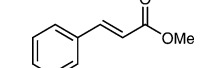
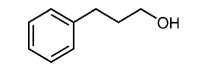
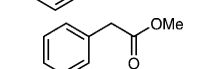
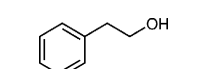
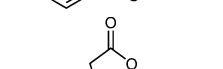
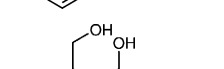
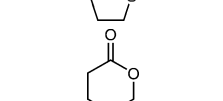
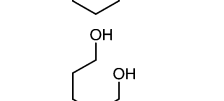
[a] Conditions: ester (10 mmol), $[\text{Ru}(\text{benzene})\text{Cl}_2]_2$ (0.25 mol%), $\mathbf{1e}$ (1 mol%), KOtBu (10 mol%), THF (10 mL), 100°C, 4.5 h, H₂ (50 bar); [b] 100°C, 2 h, H₂ (50 bar); [c] 18% monoreduction of the ester into the corresponding alcohol; [d] 13% monoreduction; [e] 100°C, 16 h, H₂ (50 bar).

chelate ring. The ruthenium center was surrounded by phosphorous, nitrogen, and chlorine atoms, as well as by the arene ligand, in a piano-stool geometry. A second chlorine atom was placed as Cl⁻ counterion. The shortest P1–Ru1

distance (2.3087(5) Å) of the cationic complexes was found in $[\text{Ru}(\text{C}_6\text{H}_6)\text{Cl}(\mathbf{1d})]\text{Cl}$. In $[\text{Ru}(\text{C}_6\text{H}_6)\text{Cl}(\mathbf{1c})]\text{Cl}$, the P1–Ru1 distance (2.3325(11) Å) was shorter than that in $[\text{Ru}(\text{C}_6\text{H}_6)\text{Cl}(\mathbf{1b})]\text{Cl}$ (2.3820(4) Å), which was in agreement with the stronger donating ability of the *t*Bu₂P moiety compared to the Cy₂P group. Figure 3d shows the ORTEP of neutral complex $[\text{Ru}(\text{C}_6\text{H}_6)\text{Cl}_2(\mathbf{1e})]$, which also exhibited a piano-stool motif. In this structure, only the phosphorous atom of ligand $\mathbf{1e}$ was coordinated to the metal center, which was unexpected coordination behavior for this type of P–N ligands.^[13] In addition, the arene ligand and two chlorine atoms completed the coordination sphere, thereby forming a neutral complex. The P1–Ru1 distance (2.3374(4) Å) was consistent with that observed in $[\text{Ru}(\text{C}_6\text{H}_6)\text{Cl}(\mathbf{1c})]\text{Cl}$ (2.3325(11) Å). This analysis was supported by MS (ESI-TOF) data: $[\text{Ru}(\text{C}_6\text{H}_6)\text{Cl}(\mathbf{1b})]\text{Cl}$, $[\text{Ru}(\text{C}_6\text{H}_6)\text{Cl}(\mathbf{1c})]\text{Cl}$, and $[\text{Ru}(\text{C}_6\text{H}_6)\text{Cl}(\mathbf{1d})]\text{Cl}$ showed signals in the positive-ion mode at $m/z = 455.09549$, 507.12655, and 495.03276, which corresponded to $[\text{Ru}(\text{C}_6\text{H}_6)\text{Cl}(\mathbf{1b})]^+$, $[\text{Ru}(\text{C}_6\text{H}_6)\text{Cl}(\mathbf{1c})]^+$, and $[\text{Ru}(\text{C}_6\text{H}_6)\text{Cl}(\mathbf{1d})]^+$, respectively, where the chlorine anion had dissociated. In the case of neutral complex $[\text{Ru}(\text{C}_6\text{H}_6)\text{Cl}_2(\mathbf{1e})]$, a signal at $m/z = 559.04162$ appeared to correspond to $[\text{Ru}(\text{C}_6\text{H}_6)\text{Cl}_2(\mathbf{1e})+\text{H}]^+$, for which both chlorine atoms were detected. To understand the different coordination behavior of ligands $\mathbf{1c}$ and $\mathbf{1e}$ in the ruthenium complexes, BP86 density functional theory (DFT) computations were performed on the molecular structures and energies of cationic bidentate monochloride complexes ($[\text{Ru}(\text{C}_6\text{H}_6)\text{Cl}(\mathbf{1c})]^+$ and $[\text{Ru}(\text{C}_6\text{H}_6)\text{Cl}(\mathbf{1e})]^+$), neutral monodentate dichloride complexes ($[\text{Ru}(\text{C}_6\text{H}_6)\text{Cl}_2(\mathbf{1c})]$ and $[\text{Ru}(\text{C}_6\text{H}_6)\text{Cl}_2(\mathbf{1e})]$), ligands $\mathbf{1c}$ and $\mathbf{1e}$, as well as the cationic $[\text{Ru}(\text{C}_6\text{H}_6)\text{Cl}]^+$ and neutral $[\text{Ru}(\text{C}_6\text{H}_6)\text{Cl}_2]$ fragments. The computational details (see the Experimental Section) and energies, as well as coordinates for all of the species investigated, are given in the Supporting Information. The computed structural parameters of the cationic $[\text{Ru}(\text{C}_6\text{H}_6)\text{Cl}(\mathbf{1c})]^+$ and neutral $[\text{Ru}(\text{C}_6\text{H}_6)\text{Cl}_2(\mathbf{1e})]$ complexes were in excellent agreement with the X-ray data, thus indicating that the computational methods were reasonable and reliable.

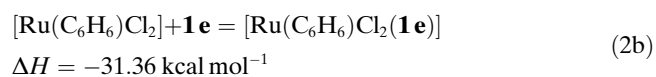
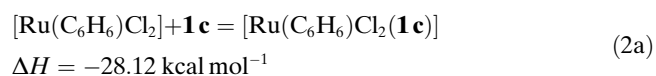
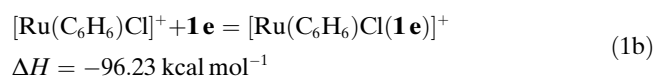
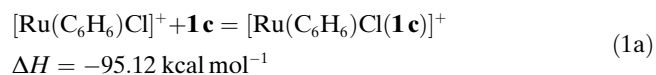
First, we compared the coordination ability of ligands $\mathbf{1c}$ and $\mathbf{1e}$ to the cationic $[\text{Ru}(\text{C}_6\text{H}_6)\text{Cl}]^+$ and neutral $[\text{Ru}(\text{C}_6\text{H}_6)\text{Cl}_2]$ fragments with the formation of the cationic ($[\text{Ru}(\text{C}_6\text{H}_6)\text{Cl}(\mathbf{1c})]^+$ and $[\text{Ru}(\text{C}_6\text{H}_6)\text{Cl}(\mathbf{1e})]^+$) and neutral complexes ($[\text{Ru}(\text{C}_6\text{H}_6)\text{Cl}_2(\mathbf{1c})]$ and $[\text{Ru}(\text{C}_6\text{H}_6)\text{Cl}_2(\mathbf{1e})]$), as shown in Equations (1) and (2). Ligand $\mathbf{1e}$ had a higher coordination energy than ligand $\mathbf{1c}$ in both the cationic bidentate and neutral monodentate complexes, by 1.11 and 3.24 kcal mol⁻¹, respectively. Additional comparisons showed that the coordination of ligand $\mathbf{1e}$ in the neutral monodentate complex was stronger than in the cationic bidentate complex and the coordination of ligand $\mathbf{1c}$ in the cationic bidentate complex was stronger than in the neutral monodentate complex. This result indicated that ligand $\mathbf{1e}$ preferred monodentate coordination, whilst ligand $\mathbf{1c}$ preferred bidentate coordination, as observed experimentally. However, the energetic difference of 2.13 kcal mol⁻¹ was rather small, and

Table 4. Catalytic hydrogenation of aliphatic esters and lactones with $[\text{Ru}(\text{benzene})\text{Cl}_2]_2/\mathbf{1c}^{\text{[a]}}$

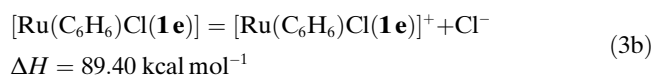
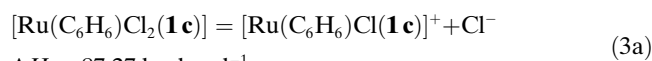
	Ester	Alcohol	Yield [%]
1			75 84 ^[b]
2			62 87 ^[b]
3			50 ^[c] 78 ^[b]
4			26 ^[c] 72 ^[d]
5			95
6			83 54 ^[e]
7			94
8			99
9			73 59 ^[e]

[a] Conditions: ester (10 mmol), $[\text{Ru}(\text{benzene})\text{Cl}_2]_2$ (0.25 mol %), $\mathbf{1c}$ (1 mol %), KOtBu (10 mol %), THF (10 mL), 100 °C, H₂ (50 bar), 4.5 h; [b] 100 °C, 16 h; [c] 120 °C, 4.5 h; [d] 120 °C, 16 h; [e] $[\text{Ru}(\text{benzene})\text{Cl}_2]_2$ (0.25 mol %), $\mathbf{1c}$ (1 mol %).

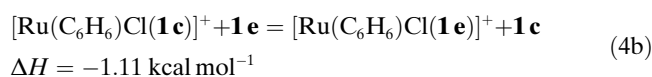
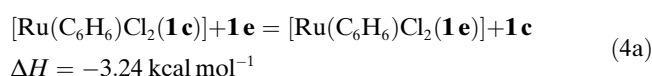
the coordination modes might have changed upon changing the reaction conditions.



In addition, we computed the heterolytic dissociation energy of a chloride anion from the neutral monodentate complexes ($[\text{Ru}(\text{C}_6\text{H}_6)\text{Cl}_2(\mathbf{1c})]$ and $[\text{Ru}(\text{C}_6\text{H}_6)\text{Cl}_2(\mathbf{1e})]$) to the cationic bidentate complexes ($[\text{Ru}(\text{C}_6\text{H}_6)\text{Cl}(\mathbf{1c})]^+$ and $[\text{Ru}(\text{C}_6\text{H}_6)\text{Cl}(\mathbf{1e})]^+$), as shown in Equation (3). Although both dissociation reactions were endothermic, the difference between the dissociation energies showed that $[\text{Ru}(\text{C}_6\text{H}_6)\text{Cl}_2(\mathbf{1e})]$ had stronger chloride coordination than $[\text{Ru}(\text{C}_6\text{H}_6)\text{Cl}_2(\mathbf{1c})]$ by 2.13 kcal mol⁻¹.



Finally, we computed the ligand-exchange energies on the basis of the reactions in Equation (4). The exchange reactions were exothermic, thus indicating that both $[\text{Ru}(\text{C}_6\text{H}_6)\text{Cl}_2(\mathbf{1e})]$ and $[\text{Ru}(\text{C}_6\text{H}_6)\text{Cl}(\mathbf{1e})]^+$ were thermodynamically favored over $[\text{Ru}(\text{C}_6\text{H}_6)\text{Cl}_2(\mathbf{1c})]$ and $[\text{Ru}(\text{C}_6\text{H}_6)\text{Cl}(\mathbf{1c})]^+$, respectively. The difference in energy (2.13 kcal mol⁻¹) revealed that $[\text{Ru}(\text{C}_6\text{H}_6)\text{Cl}_2(\mathbf{1e})]$ was more-favored compared to $[\text{Ru}(\text{C}_6\text{H}_6)\text{Cl}(\mathbf{1e})]^+$ or, in terms of the reversal reaction, $[\text{Ru}(\text{C}_6\text{H}_6)\text{Cl}_2(\mathbf{1c})]$ was less-favored than $[\text{Ru}(\text{C}_6\text{H}_6)\text{Cl}(\mathbf{1c})]^+$.



On the basis of this rather small difference in energy, and also based on the existence of $[\text{Ru}(\text{C}_6\text{H}_6)\text{Cl}_2(\mathbf{1e})]$ and $[\text{Ru}(\text{C}_6\text{H}_6)\text{Cl}(\mathbf{1e})]^+$, we expected that the cationic complex $[\text{Ru}(\text{C}_6\text{H}_6)\text{Cl}(\mathbf{1e})]^+$ should be obtainable under suitable conditions. In fact, the energy difference of the exchange from the monodentate into the bidentate coordination of ligand $\mathbf{1e}$ in solution should be very small. Because such exchange is favored by an increased entropy change, simply raising the temperature should result in such a coordination change. To confirm this assumption, variable-temperature ¹H NMR and ³¹P NMR experiments of $[\text{Ru}(\text{C}_6\text{H}_6)\text{Cl}_2(\mathbf{1e})]$ were carried out (Figure 4).

At room temperature (297 K), the ³¹P NMR spectrum shows a strong signal at $\delta = 30.5$ ppm, which was assigned to the neutral complex $[\text{Ru}(\text{C}_6\text{H}_6)\text{Cl}_2(\mathbf{1e})]$, and a small signal at $\delta = 57$ ppm, which represented the cationic species $[\text{Ru}(\text{C}_6\text{H}_6)\text{Cl}(\mathbf{1e})]\text{Cl}$. When heating the NMR tube in increments of 10 °C up to 60 °C (333 K), the peak at $\delta = 30.5$ ppm vanished whilst the signal at $\delta = 57$ ppm increased. After 2 h at 60 °C, the equilibrium shifted completely towards the cationic complex. Interestingly, after heating the cationic complex, it became stable, even at room temperature, which indicated that the neutral complex was kinetically stable but that the cationic complex was thermodynamically more-stable. A similar transformation of a neutral species into a cationic species was also observed by NMR spectroscopy of the neutral complex $[\text{Ru}(\text{C}_6\text{H}_6)\text{Cl}_2(\mathbf{1e})]$ at room temperature after 2 weeks.

Moreover, a second set of signals was observed in the ¹H NMR spectrum at room temperature, which grew during the heating process. In this case, the chemical shift of the benzene moiety was particularly suitable for investigating the transformation of the neutral complex into the cationic

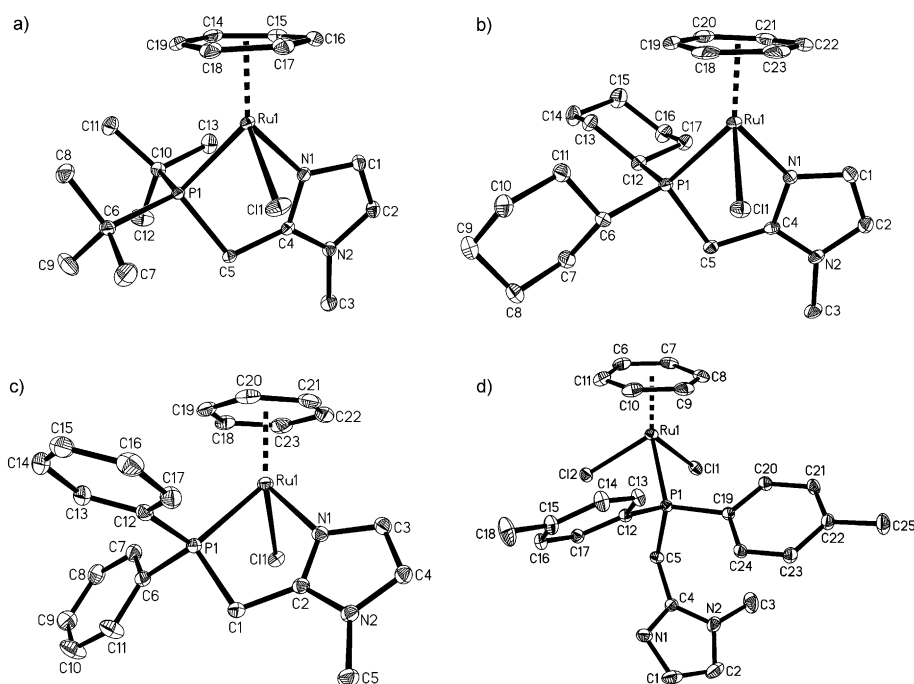


Figure 3. a) ORTEP of the cation of $[\text{Ru}(\text{C}_6\text{H}_6)\text{Cl}(\mathbf{1b})]\text{Cl}$. Hydrogen atoms are omitted for clarity; thermal ellipsoids set at 30% probability. Selected bond lengths [\AA] and angles [$^\circ$]: P1–Ru1 2.3820(4), Cl1–Ru1 2.4066(4), N1–Ru1 2.0931(11); N1–Ru1–P1 77.90(3), P1–Ru1–Cl1 89.44(1), N1–Ru1–Cl1 82.57(3). b) ORTEP of the cation of $[\text{Ru}(\text{C}_6\text{H}_6)\text{Cl}(\mathbf{1c})]\text{Cl}$. Hydrogen atoms are omitted for clarity; thermal ellipsoids set at 30% probability. Selected bond lengths [\AA] and angles [$^\circ$]: P1–Ru1 2.3325(11), Cl1–Ru1 2.4039(10), N1–Ru1 2.089(3); N1–Ru1–P1 79.62(10), P1–Ru1–Cl1 83.03(4), N1–Ru1–Cl1 83.1(1). c) ORTEP of the cation of $[\text{Ru}(\text{C}_6\text{H}_6)\text{Cl}(\mathbf{1d})]\text{Cl}$. Hydrogen atoms are omitted for clarity; thermal ellipsoids set at 30% probability. Selected bond lengths [\AA] and angles [$^\circ$]: P1–Ru1 2.3087(5), Cl1–Ru1 2.4016(5), N1–Ru1 2.079(2); N1–Ru1–P1 79.51(5), P1–Ru1–Cl1 83.74(2), N1–Ru1–Cl1 86.12(5). d) ORTEP of $[\text{Ru}(\text{C}_6\text{H}_6)\text{Cl}_2(\mathbf{1e})]$. Hydrogen atoms are omitted for clarity; thermal ellipsoids set at 30% probability. Selected bond lengths [\AA] and angles [$^\circ$]: P1–Ru1 2.3374(4), Cl1–Ru1 2.4094(5), Cl2–Ru1 2.4028(4); Cl2–Ru1–Cl1 88.172(16), P1–Ru1–Cl1 85.538(16), P1–Ru1–Cl2 84.525(15).

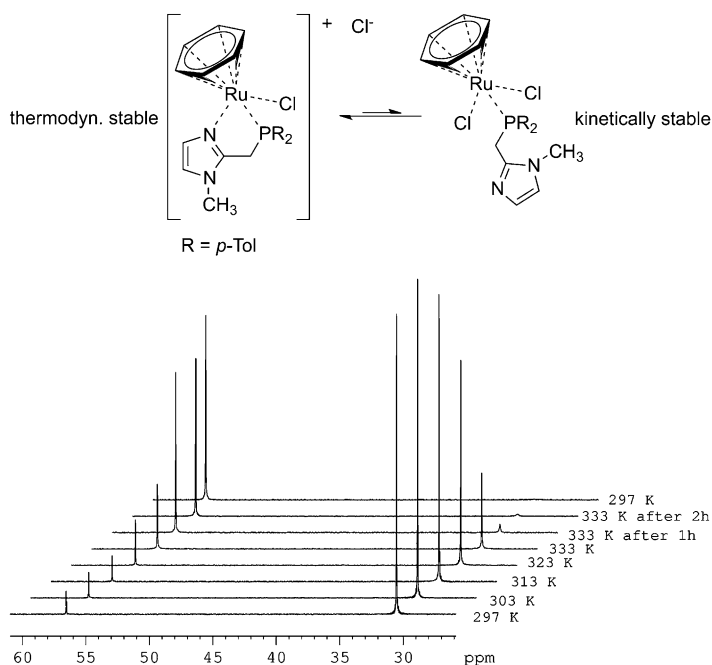


Figure 4. ^{31}P NMR spectra of $[\text{Ru}(\text{C}_6\text{H}_6)\text{Cl}_2(\mathbf{1e})]$ at different temperatures. Transformation of the neutral complex $[\text{Ru}(\text{C}_6\text{H}_6)\text{Cl}_2(\mathbf{1e})]$ into the cationic form $[\text{Ru}(\text{C}_6\text{H}_6)\text{Cl}(\mathbf{1e})]\text{Cl}$.

complex. The benzene group of $[\text{Ru}(\text{C}_6\text{H}_6)\text{Cl}_2(\mathbf{1e})]$ gave a characteristic peak at $\delta = 5.3$ ppm. An additional small signal at 5.8 ppm was found at 297 K, which was attributed to benzene in $[\text{Ru}(\text{C}_6\text{H}_6)\text{Cl}(\mathbf{1e})]\text{Cl}$. On heating the sample, the ^1H NMR spectra showed a decrease in the signal at $\delta = 5.3$ ppm whilst the peak at $\delta = 5.8$ ppm grew. Finally, the NMR sample was evaporated and investigated by MS (ESI-TOF), which showed a signal at $m/z = 523.06449$, which corresponded to the cationic $[\text{Ru}(\text{C}_6\text{H}_6)\text{Cl}(\mathbf{1e})]^+$ species, with only one chlorine atom being detected.

To determine the relative stability of the different complexes, ligand $\mathbf{1e}$ was added into a solution of complex $[\text{Ru}(\text{C}_6\text{H}_6)\text{Cl}(\mathbf{1c})]\text{Cl}$. Besides the ^{31}P NMR signal for complex $[\text{Ru}(\text{C}_6\text{H}_6)\text{Cl}(\mathbf{1c})]\text{Cl}$ ($\delta = 74.45$ ppm) and the free ligand $\mathbf{1e}$ ($\delta = -18.3$ ppm), a third peak appeared at $\delta = 30$ ppm, which corresponded to $[\text{Ru}(\text{C}_6\text{H}_6)\text{Cl}_2(\mathbf{1e})]$. Neutral complex $[\text{Ru}(\text{C}_6\text{H}_6)\text{Cl}_2(\mathbf{1e})]$ was formed by ligand exchange from the cationic complex $[\text{Ru}(\text{C}_6\text{H}_6)\text{Cl}(\mathbf{1c})]\text{Cl}$.

Based on these spectroscopic findings, different metal to ligand ratios of the in-situ-generated catalyst $[\{\text{Ru}(\text{benzene})\text{Cl}_2\}_2]/\mathbf{1e}$ were tested in the benchmark hydrogenation of methyl benzoate (Table 1, entries 20–22). The best result was obtained with a $[\text{Ru}]/\mathbf{1e}$ ratio of 1:2 (94% yield), whereas, for a metal/ligand ratio of 1:1, the reactivity was somewhat lower (74% yield). When a metal/ligand ratio of 1:4 was applied, almost no reaction took place. Finally, the use of two isolated complexes, $[\text{Ru}(\text{C}_6\text{H}_6)\text{Cl}(\mathbf{1c})]\text{Cl}$ and $[\text{Ru}(\text{C}_6\text{H}_6)\text{Cl}_2(\mathbf{1e})]$, in the reduction of methyl benzoate showed comparable activity (23–26% yield; Table 1, entries 23 and 25). When a second equivalent of ligand $\mathbf{1c}$ or $\mathbf{1e}$ was added to the respective isolated complexes, the results were similar to those with the corresponding in-situ-generated catalyst $[\{\text{Ru}(\text{benzene})\text{Cl}_2\}_2]/\mathbf{1c}$ or $[\{\text{Ru}(\text{benzene})\text{Cl}_2\}_2]/\mathbf{1e}$ (Table 1, entries 24 and 26).

Conclusion

A convenient synthesis of hemilabile P–N ligands $\mathbf{1}$ and $\mathbf{2}$ and their application in the ruthenium-catalyzed reduction

of esters is presented. The combination of $[\{\text{Ru}(\text{benzene})\text{Cl}_2\}_2]/\mathbf{1e}$ gave an active and selective catalyst for the reduction of substituted aromatic esters and lactones. On the other hand, the combination of $[\{\text{Ru}(\text{benzene})\text{Cl}_2\}_2]/\mathbf{1c}$ gave especially good results for the hydrogenation of aliphatic lactones or carboxylic esters. The scope of these in situ catalyst systems was demonstrated in the reduction of 23 esters, which generally proceeded in good yields. Furthermore, a series of ruthenium complexes with phosphine–imidazolyl ligands $[\text{Ru}(\text{C}_6\text{H}_6)\text{Cl}_2(\mathbf{1})]$ were synthesized and fully characterized to investigate the active catalyst. These complexes should also be useful in other reductions reactions, such as the reduction of nitriles,^[14] amides, etc.

Experimental Section

General procedure for the catalytic hydrogenation of esters: A mixture of $[\{\text{Ru}(\text{benzene})\text{Cl}_2\}_2]$ (0.5 mol % Ru) and ligand **1** (1 mol %) in THF (5 mL) was purged with argon in a Schlenk tube and stirred for 15 min at RT. To the in-situ-generated catalyst were added KOtBu (0.1 mmol), hexadecane (as a standard, 1 mL), and a liquid ester (10 mmol) and the mixture was stirred for a further 5 min. (If a solid ester was used, it was added directly into the autoclave.) The reaction mixture was transferred via a syringe into the autoclave (25 mL Parr autoclave), the autoclave was flushed twice with hydrogen, filled with hydrogen (50 bar), and the mixture was stirred at the required temperature (80–120 °C) for the predetermined time (4.5–16 h). The autoclave was allowed to cool to RT, the hydrogen was released, and the reaction mixture was passed through a short plug of silica gel. The yield was determined by GC (30 m HP 5 Agilent Technologies 50–300 °C).

Computational details: Structure optimizations were carried out at the BP86^[15] density functional level of theory with the SVP basis set for non-metal elements (C, H, P, N, Cl)^[16] and with the LANL2DZ basis set for Ru^[17] with the Gaussian03 program package.^[18] The optimized geometries were characterized as energy minima at the potential energy surface from frequency calculations at the same level of theory (BP86/SVP), that is, the energy-minimum structure had only real frequencies. For comparison with the X-ray structural parameters, the structures were refined with the TZVP basis set for the non-metal elements;^[19] the computed energies were used for the relative-energy discussion.

X-ray crystal-structure analysis: Diffraction data for **1a**·2HBr and **1c**·HBr were collected on a STOE IPDS II diffractometer, whilst diffraction data for $[\text{Ru}(\text{C}_6\text{H}_6)\text{Cl}(\mathbf{1b})]\text{Cl}$, $[\text{Ru}(\text{C}_6\text{H}_6)\text{Cl}(\mathbf{1e})]\text{Cl}$, $[\text{Ru}(\text{C}_6\text{H}_6)\text{Cl}(\mathbf{1d})]\text{Cl}$, and $[\text{Ru}(\text{C}_6\text{H}_6)\text{Cl}_2(\mathbf{1e})]$ were collected on a Bruker APEX II Duo; graphite-monochromated Mo K α radiation was used in all cases. The structures were solved by direct methods and refined by full-matrix least-squares procedures on F^2 with the SHELXTL software package; XP (Bruker AXS) was used for graphical representations.^[20] CCDC-865729 (**1a**·2HBr), CCDC-865728 (**1c**·HBr), CCDC-865726 ($[\text{Ru}(\text{C}_6\text{H}_6)\text{Cl}(\mathbf{1b})]\text{Cl}$), CCDC-865724 ($[\text{Ru}(\text{C}_6\text{H}_6)\text{Cl}(\mathbf{1e})]\text{Cl}$), CCDC-865727 ($[\text{Ru}(\text{C}_6\text{H}_6)\text{Cl}(\mathbf{1d})]\text{Cl}$), CCDC-865725 ($[\text{Ru}(\text{C}_6\text{H}_6)\text{Cl}_2(\mathbf{1e})]$) contain the supplementary crystallographic data for this paper. These data can be obtained free of charge from The Cambridge Crystallographic Data Centre via www.ccdc.cam.ac.uk/data_request/cif.

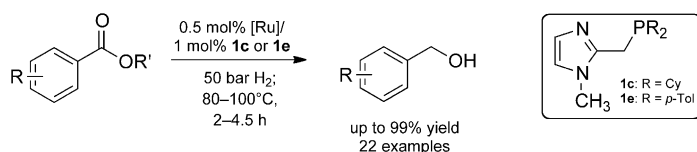
Acknowledgements

We thank Dr. C. Fischer, S. Buchholz, S. Schareina, and S. Rossmesl (all at the Leibniz-Institut für Katalyse e.V.) for their excellent analytical and technical support. Special thanks go to Dr. W. Baumann and A. Koch for the variable-temperature NMR spectroscopy measurements.

- [1] a) P. N. Rylander, *Catalytic Hydrogenation in Organic Syntheses*, Academic Press, New York, **1979**; b) *Handbook of Heterogeneous Hydrogenation for Organic Synthesis* (Ed.: S. Nishimura), Wiley, New York, **2001**; c) *Handbook of Homogeneous Hydrogenation* (Eds.: J. G. de Vries, C. J. Elsevier), Wiley-VCH, Weinheim, **2007**; d) P. G. Andersson, I. J. Munslow, *Modern Reduction Methods*, Wiley, New York, **2008**.
- [2] a) L. Saudan in *Applied Homogeneous Catalysis with Organometallic Compounds: A Comprehensive Handbook in Three Volumes* (Eds.: B. Cornils, W. A. Herrmann, M. Beller, R. Paciello), Wiley-VCH, Weinheim, **2012**, in press; b) M. L. Clarke, G. J. Roff, *The Handbook of Homogeneous Hydrogenation* (Eds.: J. G. de Vries, C. J. Elsevier), Wiley-VCH, Weinheim, **2007**, pp. 313–454; c) M. Ito, T. Ikariya, *Chem. Commun.* **2007**, 5134–5142.
- [3] For the catalytic reduction of carboxylic acids, see: a) M. Bianchi, G. Menchi, F. Francalanci, F. Piacenti, U. Matteoli, P. Frediani, C. Botteghi, *J. Organomet. Chem.* **1977**, *141*, 107–111; b) M. Bianchi, G. Menchi, F. Francalanci, F. Piacenti, U. Matteoli, P. Frediani, C. Botteghi, *J. Organomet. Chem.* **1980**, *188*, 109–119; c) D. He, N. Wakasa, T. Fuchikami, *Tetrahedron Lett.* **1995**, *36*, 1059–62.
- [4] For the catalytic reduction of amide derivatives, see: a) A. A. Núñez Magro, G. R. Eastham, D. J. Cole-Hamilton, *Chem. Commun.* **2007**, 3154–3156; b) E. Balaraman, B. Gnanaprakasam, L. J. W. Shimon, D. Milstein, *J. Am. Chem. Soc.* **2010**, *132*, 16756–16758; c) M. Ito, T. Ootsuka, R. Watari, A. Shiibashi, A. Himizu, T. Ikariya, *J. Am. Chem. Soc.* **2011**, *133*, 4240–4242; d) J. M. John, S. H. Bergens, *Angew. Chem.* **2011**, *123*, 10561–10564; *Angew. Chem. Int. Ed.* **2011**, *50*, 10377–10380; e) E. Balaraman, Y. Ben-David, D. Milstein, *Angew. Chem.* **2011**, *123*, 11906–11909; *Angew. Chem. Int. Ed.* **2011**, *50*, 11702–11705. For the catalytic reduction of imide derivatives, see: f) R. Aoun, J.-L. Renaud, P. H. Dixneuf, C. Bruneau, *Angew. Chem.* **2005**, *117*, 2057–2059; *Angew. Chem. Int. Ed.* **2005**, *44*, 2021–2023; g) M. Ito, A. Sakaguchi, C. Kobayashi, T. Ikariya, *J. Am. Chem. Soc.* **2007**, *129*, 290–291.
- [5] a) R. A. Grey, G. P. Pez, A. Wallo, J. Corsi, *Chem. Commun.* **1980**, 783–784; b) A. R. Grey, G. P. Pez, A. Wallo, *J. Am. Chem. Soc.* **1981**, *103*, 7536–7542; c) U. Matteoli, M. Bianchi, G. Menchi, P. Prediani, F. Piacenti, *J. Mol. Catal.* **1984**, *22*, 353–362; d) U. Matteoli, G. Mechi, M. Bianchi, F. Piacenti, *J. Organomet. Chem.* **1986**, *299*, 233–238; e) U. Matteoli, G. Menchi, M. Bianchi, F. Piacenti, *J. Mol. Catal.* **1988**, *44*, 347–355; f) U. Matteoli, G. Mechi, M. Bianchi, F. Piacenti, S. Ianelli, M. Nardelli, *J. Organomet. Chem.* **1995**, *498*, 177–186; g) J. Zhang, G. Leitius, Y. Ben-David, D. Milstein, *Angew. Chem.* **2006**, *118*, 1131–1133; *Angew. Chem. Int. Ed.* **2006**, *45*, 1113–1115; h) L. A. Saudan, C. M. Saudan, C. Debieux, P. Wyss, *Angew. Chem.* **2007**, *119*, 7617–7620; *Angew. Chem. Int. Ed.* **2007**, *46*, 7473–7476; i) M. L. Clarke, M. B. Diaz-Valenzuela, A. M. Z. Slawin, *Organometallics* **2007**, *26*, 16–19; j) Y. Sun, C. Koehler, R. Tan, V. T. Annibale, D. Song, *Chem. Commun.* **2011**, *47*, 8349–8351; k) E. Fogler, E. Balaraman, Y. Ben-David, G. Leitius, L. J. W. Shimon, D. Milstein, *Organometallics* **2011**, *30*, 3826–3833; l) E. Balaraman, E. Fogler, D. Milstein, *Chem. Commun.* **2012**, *48*, 1111–1113.
- [6] For the in situ formation of a $[\text{Ru}(\text{acac})_3]$ /phosphine catalyst, see: a) Y. Hara, H. Inagaki, S. Nishimura, K. Wada, *Chem. Lett.* **1992**, 1983–1986; b) H. T. Teunissen, C. J. Elsevier, *Chem. Commun.* **1997**, 667–668; c) H. T. Teunissen, C. J. Elsevier, *Chem. Commun.* **1998**, 1367–1367; d) K. Nomura, H. Ogura, Y. Imanishi, *J. Mol. Catal. A: Chem.* **2001**, *166*, 345–349; e) M. C. Van Engelen, H. T. Teunissen, J. G. de Vries, C. J. Elsevier, *J. Mol. Catal. A: Chem.* **2003**, *206*, 185–192; f) M. J. Hanton, S. Tin, B. J. Boardman, P. Miller, *J. Mol. Catal. A: Chem.* **2011**, *346*, 70–78.
- [7] a) S. Zhou, K. Junge, D. Addis, S. Das, M. Beller, *Angew. Chem.* **2009**, *121*, 9671–9674; *Angew. Chem. Int. Ed.* **2009**, *48*, 9507–9510; b) S. Zhou, D. Addis, S. Das, K. Junge, M. Beller, *Chem. Commun.* **2009**, 4883–4885; c) S. Zhou, K. Junge, D. Addis, S. Das, M. Beller, *Org. Lett.* **2009**, *11*, 2461–2464; d) S. Das, D. Addis, S. Zhou, K. Junge, M. Beller, *J. Am. Chem. Soc.* **2010**, *132*, 1770–1771; e) S. Das, S. Zhou, D. Addis, S. Enthaler, K. Junge, M. Beller, *Top. Catal.*

- 2010, 53, 979984; f) D. Addis, S. Das, K. Junge, M. Beller, *Angew. Chem.* **2011**, 123, 6128–6135; *Angew. Chem. Int. Ed.* **2011**, 50, 6004–6011; g) S. Das, K. Möller, K. Junge, M. Beller, *Chem. Eur. J.* **2011**, 17, 7414–7417; h) S. Das, D. Addis, L. R. Knöpke, U. Bendrup, K. Junge, A. Brückner, M. Beller, *Angew. Chem.* **2011**, 123, 9346–9359; *Angew. Chem. Int. Ed.* **2011**, 50, 9180–9184; i) S. Das, D. Addis, K. Junge, M. Beller, *Chem. Eur. J.* **2011**, 17, 12186–12192; j) S. Das, B. Join, K. Junge, M. Beller, *Chem. Commun.* **2012**, 48, 2683–2685.
- [8] a) M. A. Jalil, S. Fujinami, H. Senda, H. Nishikawa, *J. Chem. Soc. Dalton Trans.* **1999**, 1655–1661; b) M. A. Jalil, S. Fujinami, H. Nishikawa, *J. Chem. Soc. Dalton Trans.* **1999**, 3499–3505; c) M. A. Jalil, S. Fujinami, H. Nishikawa, *J. Chem. Soc. Dalton Trans.* **2001**, 1091–1098; d) M. A. Jalil, E. B. Hui, *Tetrahedron Lett.* **2006**, 47, 1473–1475; e) L. D. Field, B. A. Messerle, K. Q. Vuong, P. Turner, *Dalton Trans.* **2009**, 3599–3614.
- [9] For further examples of imidazole-based P-N ligands, see: a) M. Abdul Jalil, T. Yamada, S. Fujinami, T. Honjo, H. Nishikawa, *Polyhedron* **2001**, 20, 627–633; b) G. Espino, F. A. Jalón, M. Maestro, B. R. Manzano, M. Pérez-Manrique, A. C. Bacigalupe, *Eur. J. Inorg. Chem.* **2004**, 2542–2552; c) C. Tejel, M. A. Ciriano, S. Jiménez, L. A. Oro, C. Graiff, A. Tiripicchio, *Organometallics* **2005**, 24, 1105–1111; for tridentate imidazolyl ligands: d) N. Braussaud, T. Rütther, K. J. Cavell, B. W. Skelton, A. H. White, *Synthesis* **2001**, 4, 0626–0632; e) T. Rütther, M. C. Done, K. J. Cavell, E. J. Peacock, B. W. Skelton, A. H. White, *Organometallics* **2001**, 20, 5522–5531.
- [10] (1-Methyl-1-H-imidazol-2-yl)methanamine (**3**) was purchased from Aldrich. For a synthetic procedure, see: S. Price, R. Bull, S. Cramo, S. Garden, M. v. d. Heuvel, D. Neigjbour, S. E. Osbourn, I. J. P. de Esch, C. L. Buenemann, *Tetrahedron Lett.* **2004**, 45, 5581–5583.
- [11] a) K. Junge, B. Hagemann, S. Enthaler, G. Oehme, M. Michalik, A. Monsees, T. Riermeier, U. Dingerdissen, M. Beller, *Angew. Chem.* **2004**, 116, 5176–5179; *Angew. Chem. Int. Ed.* **2004**, 43, 5066–5069; b) B. Hagemann, K. Junge, S. Enthaler, M. Michalik, T. Riermeier, A. Monsees, M. Beller, *Adv. Synth. Catal.* **2005**, 347, 1978–1986.
- [12] Methyl-4-cyanobenzoate was reduced with $[[\text{Ru}(\text{benzene})\text{Cl}_2]_2]/\mathbf{1c}$ to give methyl-4-(aminomethyl)benzoate (51%) and 4-(hydroxymethyl)benzotrile (13% yield). The reduction of methyl-4-acetylbenzoate with $[[\text{Ru}(\text{benzene})\text{Cl}_2]_2]/\mathbf{1e}$ afforded methyl 4-(1-hydroxyethyl)benzoate in 58% yield.
- [13] Crystal structures of Ni-, Mo-, Ir-, Rh-, and Pd complexes of ligands **1a** and **1d** are reported;^[8a,b,c,e] in these cases, the P-N ligands were always coordinated as bidentate species.
- [14] For selected recent examples of the ruthenium-catalyzed hydrogenation of nitriles, see: a) T. Li, I. Bergner, F. N. Haque, M. Zimmer-De Iulius, D. Song, R. H. Morris, *Organometallics* **2007**, 26, 5940–5949; b) S. Enthaler, D. Addis, K. Junge, G. Erre, M. Beller, *Chem. Eur. J.* **2008**, 14, 9491–9494; c) S. Enthaler, K. Junge, D. Addis, G. Erre, M. Beller, *ChemSusChem* **2008**, 1, 1006–1010; d) D. Addis, S. Enthaler, K. Junge, B. Wendt, M. Beller, *Tetrahedron Lett.* **2009**, 50, 3654–3656; e) R. Reguillo, M. Grellier, N. Vautravers, L. Vendier, S. Sabo-Etienne, *J. Am. Chem. Soc.* **2010**, 132, 7854–7855; f) C. Gunanathan, M. Hölscher, W. Leitner, *Eur. J. Inorg. Chem.* **2011**, 3381–3386.
- [15] J. P. Perdew, *Phys. Rev. B* **1986**, 33, 8822–8824.
- [16] A. Schäfer, H. Horn, R. Ahlrichs, *J. Chem. Phys.* **1992**, 97, 2571–77.
- [17] P. J. Hay, W. R. Wadt, *J. Chem. Phys.* **1985**, 82, 299–310.
- [18] Gaussian 03, Revision D.02, M. J. Frisch, G. W. Trucks, H. B. Schlegel, G. E. Scuseria, M. A. Robb, J. R. Cheeseman, J. A. Montgomery, Jr., T. Vreven, K. N. Kudin, J. C. Burant, J. M. Millam, S. S. Iyengar, J. Tomasi, V. Barone, B. Mennucci, M. Cossi, G. Scalmani, N. Rega, G. A. Petersson, H. Nakatsuji, M. Hada, M. Ehara, K. Toyota, R. Fukuda, J. Hasegawa, M. Ishida, T. Nakajima, Y. Honda, O. Kitao, H. Nakai, M. Klene, X. Li, J. E. Knox, H. P. Hratchian, J. B. Cross, V. Bakken, C. Adamo, J. Jaramillo, R. Gomperts, R. E. Stratmann, O. Yazyev, A. J. Austin, R. Cammi, C. Pomelli, J. W. Ochterski, P. Y. Ayala, K. Morokuma, G. A. Voth, P. Salvador, J. J. Dannenberg, V. G. Zakrzewski, S. Dapprich, A. D. Daniels, M. C. Strain, O. Farkas, D. K. Malick, A. D. Rabuck, K. Raghavachari, J. B. Foresman, J. V. Ortiz, Q. Cui, A. G. Baboul, S. Clifford, J. Cioslowski, B. B. Stefanov, G. Liu, A. Liashenko, P. Piskorz, I. Komaromi, R. L. Martin, D. J. Fox, T. Keith, M. A. Al-Laham, C. Y. Peng, A. Nanayakkara, M. Challacombe, P. M. W. Gill, B. Johnson, W. Chen, M. W. Wong, C. Gonzalez, J. A. Pople, Gaussian, Inc., Wallingford CT, **2004**.
- [19] A. Schäfer, C. Huber, R. Ahlrichs, *J. Chem. Phys.* **1994**, 100, 5829–5835.
- [20] G. M. Sheldrick, *Acta Cryst.* **2008**, A64, 112–122.

Received: February 7, 2012
Published online: ■ ■ ■, 0000



P–N the tail on the donkey: The combination of [[Ru(benzene)Cl₂]₂] and P–N ligand **1e** was active in the hydrogenation of aromatic esters and lactones,

whilst [[Ru(benzene)Cl₂]₂]/**1c** attained good results in the reduction of aliphatic lactones and esters (see scheme).

Ru Catalysis

*K. Junge, B. Wendt, F. A. Westerhaus,
A. Spannenberg, H. Jiao,
M. Beller**



Phosphine–Imidazolyl Ligands for the Efficient Ruthenium-Catalyzed Hydrogenation of Carboxylic Esters

